https://doi.org/10.5194/tc-2019-192
Preprint. Discussion started: 26 August 2019

The Cryosphere Discussions

Multidecadal Arctic sea ice thickness and volume derived from ice age

Yinghui Liu[1], Jeffrey R. Key[1], Xuanji Wang[2], and Mark Tschudi[3]

[1]Center for Satellite Applications and Research, NOAA/NESDIS, Madison, Wisconsin
[2]Cooperative Institute of Meteorological Satellite Studies, University of Wisconsin, Madison, WI
[3]Colorado Center for Astrodynamics Research, University of Colorado, Boulder, CO

Correspondence to: Yinghui Liu (Yinghui.Liu@noaa.gov)

Abstract. Arctic sea ice is a key component of the Arctic climate system, which in turn impacts global climate. Ice concentration, thickness, and volume are among the most important Arctic sea ice parameters. This study presents a new record of Arctic sea ice thickness and volume from 1984 to 2018 based on an existing satellite-derived ice age product. The relationship between ice age and ice thickness is first established for every month based on collocated ice age and ice thickness from submarine sonar data (1984-2000), the Ice, Cloud, and land Elevation Satellite (ICESat, 2003-2008), and an empirical ice growth model. Based on this relationship, ice thickness is derived for the entire time period from the weekly ice age product, and the Arctic monthly sea ice volume is then calculated. The ice age-based thickness and volume show good agreement in terms of bias and root mean square error with submarine, ICESat, and CryoSat-2 ice thickness, as well as ICESat and CryoSat-2 ice volume, in February/March and October/November. Sea ice volume exhibits a decreasing trend of -411 km^3/year from 1984 to 2018, stronger than the trends from other datasets. Of the factors affecting volume, changes in sea ice thickness from November to May contribute at least 80%, decreasing to around 50% in August and September. Changes in sea ice area contribute less than 30% in all months.

1 Introduction

Sea ice plays a key role in regulating the energy and mass exchange between the atmosphere and the underlying ocean in the polar regions. Over the last few decades Arctic sea ice extent, area, thickness, and volume have declines significantly (Stroeve et al. 2012, Kwok 2019). The accompanying surface albedo decreases and cloud property changes lead to additional surface radiation absorption, which results in further sea ice reduction (Letterly et al. 2018, Perovich et al. 2007, Pistone et al. 2014). The anomalous sea ice export out of the Arctic Ocean affects the strength of the Atlantic Meridional Overturning Circulation, and thus global climate (Sévellec et al. 2017). Arctic sea ice volume is likely a more sensitive climate change index than ice extent and area in that the reduction in Arctic sea ice volume is as much as two times that of sea ice extent on a percentage basis in global climate model simulations (Gregory et al. 2002). Thus, monitoring Arctic sea ice extent, area,

https://doi.org/10.5194/tc-2019-192
Preprint. Discussion started: 26 August 2019

thickness, and volume is becoming increasingly important in understanding the Arctic and global climate systems and their changes, and improving climate forecasting.

Using satellites to estimate sea ice properties is advantageous because of the much higher spatial and temporal coverage in the polar regions compared to in situ observations. Uncertainty in satellite-derived Arctic sea ice extent and area is low overall due to the relatively high quality of sea ice concentration retrievals from satellite passive microwave data. Available since the late 1970s, multiple passive microwave sea ice concentration products have provided valuable information in studying trends for sea ice extent and area in the polar regions (Ivanova et al. 2015). Sea ice concentrations from satellite sensors in the visible and infrared spectrum have the potential to provide additional information owing to their higher spatial resolution (Liu et al. 2016).

Sea ice thickness products have been generated with space-based lidar and radar altimeters onboard the Ice, Cloud, and land Elevation Satellite (ICESat) and CryoSat-2 respectively (Kwok et al. 2009, Laxon et al. 2013), from passive visible and infrared radiometers using the One-dimensional Thermodynamic Ice Model (OTIM) (Wang et al. 2010), from the Soil Moisture and Ocean Salinity (SMOS) satellite, and from other passive microwave radiometers (Tian-Kunze et al. 2014). Sea ice thickness products will also be available from ICESat-2 in the near future (Kwok et al. 2016, Markus et al. 2017). The lidar and radar altimeter and SMOS sea ice thickness products cover from the early and late 2000s respectively, while OTIM ice thickness products cover 1982 to the present using the Advanced Very High Resolution Radiometer (AVHRR) on NOAA polar-orbiting satellites.

Sea ice thickness is not a physical parameter that satellite visible and infrared sensors can observe directly. Statistical models or physically based thermodynamic models with numerical parameterizations are needed to retrieve ice thickness with satellite observations (Wang et al. 2010, Kwok et al. 2016, Tian-Kunze et al. 2014). The underlying physical processes controlling ice growth and melting are so complex that uncertainties in the parameterizations in those models lead to large uncertainties in the ice thickness products. For example, the depth of snow on sea ice is a critical parameter for all the ice thickness retrieval methods, and yet, currently, there is no way to accurately measure it from space (e.g. Wang et al. 2010).

In addition to these satellite ice thickness products, sea ice thickness is also available from regional and global numerical models, e.g. the Pan-Arctic Ice-Ocean Modeling and Assimilation System (PIOMAS) (Zhang and Rothrock 2003, Schweiger et al. 2011, 2019, Lindsay et al., 2012, Laxon et al. 2013), and global climate models. Although the global climate models tend to underestimate the rate of ice volume loss and represent the thickness spatial patterns poorly, multi-model ensemble means provide realistic trends (Stroeve et al. 2014).

Sea ice thickness can also be derived from sea ice age. An Arctic sea ice age product covering the period from 1984 to the present has been generated based on Lagrangian tracking of individual sea ice (Tschudi et al. 2019a). Studies have shown that a generally linear relationship exists between the ice age and the ICESat sea ice thickness from 2003 to 2008 (Maslanik et al. 2007, Tschudi et al. 2016), and such a relationship has been applied to estimate the sea ice thickness in March extending back to the early 1980s (Maslanik et al. 2007). However, the way in which the relationship between age and thickness varies over the course of the year and over the multi-decadal time series was not considered in that work. If sea ice

https://doi.org/10.5194/tc-2019-192
Preprint. Discussion started: 26 August 2019

thickness and sea ice age relationships are available for all months of the ice age dataset, a more robust ice thickness dataset can be created. To establish the relationship between age and thickness in the earlier years, we use Arctic sea ice draft data that have been collected by naval submarines since 1958, with data from 1975 to 2000 publicly available (Rothrock et al. 2008, NSIDC 1998). Furthermore, ice thickness can be combined with ice concentration data to produce a new ice volume product.

This paper presents Arctic Ocean sea ice thickness and volume from 1984 to 2018 based on an existing sea ice age product. Relationships between ice age and ice thickness are established for all months 1984-2018. Weekly ice thickness is then produced based on the weekly ice age product, followed by the calculation of monthly ice volume. Spatial distributions and temporal trends of the derived sea ice thickness and volume are presented. The ice age-based thickness and volume data set from 1984 to 2018 is also compared to existing data sets.

2 Data and Methods

2.1 Data

A weekly sea ice age product from 1984 to 2018 has been generated (Tschudi et al. 2019a) and is available from the National Snow and Ice Data Center (NSIDC, Boulder, Colorado, USA). The ice age category represents how long in years the sea ice has existed since its first appearance, which is estimated through Lagrangian tracking of the ice from week to week using gridded ice motion vectors (Masnalik et al. 2007, Maslanik et al. 2011, Tschudi et al. 2019a). The weekly ice motion vectors are generated by merging the ice motion vectors from passive visible/infrared and microwave sensors, International Arctic Buoy Program (IABP) buoys, and NCEP/NCAR Reanalysis. Since late 1978, ice age has been estimated by tracking each grid cell with ice as a discrete, independent Lagrangian parcel advected by the weekly ice motions. The oldest age of a single grid cell of parcels with different ages is assigned to this parcel (Maslanik et al. 2011, Tschudi et al. 2019a). A parcel's age gains a year if it survives the summer minimum sea ice extent, which means that the ice concentration of a grid cell remains at or above 15% throughout the melt season. With each weekly file, an ice age value ranging from 1 up to 16 (years since its first appearance) is assigned to each of 722 by 722 grid cells corresponding to the 12.5 km Equal-Area Scalable Earth Grid (EASE-Grid) covering the Arctic. We used the weekly ice age products from 1984 to 2018 in this study (Tschudi et al., 2019b). Any ice age older than four years is classified as one ice age group in this scheme.

Monthly sea ice concentration from 1984 to 2017 and daily data in 2018 that were produced with the NASA Team algorithm at 25 km polar stereographic grid were obtained from NASA's Distributed Active Archive Center (DAAC) at NSIDC (Cavalieri et al. 1996). Monthly sea ice concentrations for 2018 are calculated from the daily data. Monthly mean sea ice thickness and volume data 1984-2018 from PIOMAS version 2.1 (Zhang and Rothrock, 2003, Schweiger et al. 2011) are used. PIOMAS couples the Parallel Ocean Program with a 12-category thickness and enthalpy distribution sea ice model in a generalized orthogonal curvilinear coordinate (GOCC) system; PIOMAS also has the capability of capturing the basic upper-ocean circulation features in the polar regions and of assimilating some observations. Boundary inputs at 45 degrees North

https://doi.org/10.5194/tc-2019-192
Preprint. Discussion started: 26 August 2019

come from a global ocean model. Sea ice concentration from passive microwave measurements and sea surface temperature from the NCEP/NCAR Reanalysis are assimilated in the system, with atmospheric drivers from the NCEP/NCAR Reanalysis including wind, surface air temperature, and cloud cover (Schweiger et al. 2011). Monthly mean ice thickness data from 1978 are available in a generalized curvilinear coordinate system covering 45 degrees North poleward with a grid size of 360 by 120.

U.S. Navy submarines have collected upward looking sonar (ULS) sea ice draft data in the Arctic Ocean since 1958. Originally classified, the data have been declassified and released according to set guidelines, which include restrictions that positions of the data must be rounded to the nearest 5 minutes of latitude and longitude, the date is to be rounded to the nearest third of a month, and the data are within an irregular polygon in the Arctic Ocean (NSIDC 1998). Submarine data were also collected in the SCience ICe EXercise (SCICEX) program. The SCICEX data are not classified so that the precise location and date are available. All the data are processed to provide ice draft profiles in segments and derived statistics of each segment, including ice draft characteristics (e.g., mean draft thickness), leads, etc. The submarine data from 1984 to 2000 are used here, including data from SCICEX93, SCICEX96, SCICEX97, SCICEX98, and SCICEX99 (Figure 1). The irregular polygon outlining the data release area (DRA) is shown in Figure 1.

Rothrock et al. (2008, hereinafter RPW08) analyzed these submarine data, and studied the annual cycle of the ice thickness and interannual change in the mean ice thickness. The ice draft, which is the thickness of the ice below the waterline, is converted to total ice thickness using the equation:

$$T = 1.107D - f(\tau) \quad (1)$$

where T and D are ice and ice draft thickness respectively, and $f(\tau)$ is the snow ice equivalent as a function of decimal fraction of the year τ. This conversion approach is the same as equation 3 in RPW08. The monthly mean $f(\tau)$ can be found in Table 4 in RPW08 and is also listed in Table A1 of the Appendix here.

The interannual change with the annual cycle superimposed in averaged ice thickness over the SCICEX box is derived using:

$$T = 1.107[\bar{D} + I(t-1988) - \bar{I} + A(\tau)] - \bar{f} \quad (2)$$

where $\bar{D}$ is 2.97 m, t is the year, and $\bar{f}$ (0.076) is the annual mean of $f(\tau)$, and $\bar{I}$ (−0.12 m) is the mean of I.

$$I(t-1988) = I_1(t-1988) + I_2(t-1988)^2 + I_3(t-1988)^3 \quad (3)$$

where I_1=-0.0748, I_2=-0.00219, and I_3=0.000246.

$$A(\tau) = A_{S0}\sin(2\pi\tau) + A_{C0}\cos(2\pi\tau) \quad (4)$$

where A_{s0}=0.465, A_{c0}=−0.250. Taken from RPW08, these equations will be used in the results section. Rothrock and Wensnahan (2007) determined a positive bias of 0.29 m in the ice thickness derived from submarine ULS data, and suggested a bias correction. In this study, we therefore reduce individual ice thickness observations and area mean ice thickness by 0.29 m.

Ice thickness and volume values from Kwok (2018, hereinafter RK18) are used in this study. In particular, we used the average Arctic sea ice volume and ice thickness from ICESat in February and March 2004 to 2008, and in October and

https://doi.org/10.5194/tc-2019-192
Preprint. Discussion started: 26 August 2019

November 2003 to 2007, as well as CryoSat-2 Arctic sea ice volume and thickness in February and March, and in October and November from 2011 to 2018 (Figure 2 and 3 in RK18).

Sea ice thickness data generated by OTIM with AVHRR data covers 1982 to the present, and is included in the AVHRR Polar Pathfinder-extended (APP-x) dataset (Key, et al., 2016). The OTIM ice thickness data are for both poles at a 25 EASE2 Grid on a twice daily basis. Initially based on the surface energy balance at thermal-equilibrium at the interface between the atmosphere and the ice, which may or may not be covered by snow (Wang et al. 2010), the OTIM has gradually evolved into a physical-statistical hybrid model that contains all components of the surface energy budget to estimate sea/lake/river ice thickness. Two parameterization schemes of ice thermal-dynamic and physical-dynamic processes have recently been added to account for ice growing/melting and ice rafting/hummocking processes. It should be noted that the OTIM ice thickness estimates are not available when the solar zenith angle is greater than 85 degrees and less than 91 degrees due to large uncertainties in the input surface albedo, cloud mask, and surface shortwave radiation, or when the ice surface temperature is greater than the freezing point. The accuracy of the input parameters – including snow depth, surface humidity, temperature, and wind – can significantly impact the accuracy of ice thickness calculations. Validation studies of OTIM ice thickness were performed with sea ice thickness measurements from ULS on submarines and moorings, as well as ground measurements. The overall accuracy (mean absolute bias) and uncertainty (root-mean-square difference, RMS) of the OTIM estimated ice thickness is approximately 0.20 m (less than 20%) and 0.54 m, respectively, over all types of sea ice (Wang et al., 2010, 2016).

2.2 Method

The first step is to establish the relationship between ice age and thickness for the times between 1984 and 2018 when the ice age thickness data are available. The relationships are derived first in two months of a year, April and September from 1984 to 2000 using submarine ice thickness data, and March and October from 2004 to 2008 using ICESat ice thickness data. Ice draft thickness of each segment is converted to ice thickness using Eq. 1, and the middle point of each segment is remapped to the 12.5 km EASE-Grid to match the ice age data. Each ice draft profile segment is collocated with its surrounding nine ice age values in the corresponding weekly ice age product. For ice draft profiles not from SCICEX, because of the restrictions on revealing the exact date, their observational dates are assigned to day 5, 15, or 25 when they are in the first, second, and third ten days of a month, respectively; we collocate each ice draft profile segment with its surrounding nine ice age values from its corresponding weekly ice age product, as well as the week before and after, for a total of 27 ice age values. The final ice age is determined as the age at the center of the nine points if it has the same ice age as the majority (>60%) of the nine (27) ice age samples for SCICEX. Otherwise, no ice age is determined. All matched ice thickness and age samples for individual months are recorded. Matched ice thickness and age samples in a month within a 10-year moving window (to increase the number of samples) are used to derive the relationship of ice age and ice thickness in each month at the fifth of the ten years. Only ice draft profile segments longer than 15 km are included; changing the threshold to 10 km, however, does not change the overall relationship. For each ice age category, a relationship is derived if the number of

https://doi.org/10.5194/tc-2019-192
Preprint. Discussion started: 26 August 2019

samples in a month is greater than 40. For example, we started with data in April/September from 1984 to 1993 to obtain the relationship in April (September) for 1988, and ended with data in April (September) from 1991 to 2000 to obtain the relationship in April (September) for 1995. Because the submarine measurements are concentrated in the spring and autumn, meaningful relationships are determined only in April and September.

Using the collocated ice age and thickness from ICESat over the period 2004 to 2008, Tschudi et al. (2016) derived the relationship between the two for February through April over the Arctic Ocean. We assign this relationship to the month of March. According to Figure 2 in RK18, the mean ice thickness in October and November is approximately 0.7 m less than the mean in February and March. Therefore, in October we assign the relationship of ice age and ice thickness the same as that in March except that ice thickness in each age category is 0.70 m less.

Figure 2 shows the relationship between ice age and ice thickness in April and September from 1988 to 1995 using submarine measurements, and in March and October from 2004 to 2008 using ICESat data from Tschudi et al. (2016). Older sea ice is generally thicker than younger ice, except that ice more than four years old is slightly thinner than four year old ice based on submarine measurements before 2000. This phenomenon was observed in one (2008) of five years (2004-2008) using ICESat data (Tschudi et al. 2016), but it is persistent in most years from 1988 to 1995 in the submarine data. Since 1984, for every ice age category, sea ice thickness has been generally decreasing. As in Tschudi et al. (2016), we use linear regression to derive the relationship between ice age and thickness for ice ages from one to four years, while keeping the relationship for ice older than four years. Then linear regression on ice thickness from 1988 to 1996 is used to smooth the ice thickness in each age category.

Relationships between ice age and thickness for every month are needed to convert the weekly ice age data into ice thickness. Though we have such relationships in two months of every year from 1988 to 1995, and from 2004 to 2008, relationships for all other months are needed. For this purpose, we apply an empirical model to the annual cycle of ice thickness. In this model, ice thickness increases linearly from September to the following May and decreases linearly from May to September in each sea ice category (Figure 3). The selection of September and May is consistent with the fact that the surface has a flux gain from the atmosphere from May to September, and a flux loss to the atmosphere from September to the following May (Serreze et al. 2007). From May to September the increase/decrease in sea ice thickness can be approximated by

$$T = G \times M + H_1 \quad (5)$$

where T is monthly mean ice thickness, G is the growth rate with units of m/month, M is month index from May to September, and H_1 is a constant (m). From September to the following May,

$$T = D \times M + H_2 \quad (6)$$

where T is monthly mean ice thickness, D is growth/declining rate with unit of m/month, M is month index from September to the following May, and H_2 is a constant (m). Given that both equations provide the same results for both September and May, and the known relationship of ice age and thickness in April and September from 1988 to 1996, as well as in March

https://doi.org/10.5194/tc-2019-192
Preprint. Discussion started: 26 August 2019

and October from 2004 to 2008, we derive G, D, H_1, and H_2, thereby determining the relationship between ice age and thickness for every month in those years following Eqs. 5 and 6. For the years before 1988 and after 2008, we use the relationship for 1988 and 2008; for years from 1996 to 2003, we derive the relationship using linear interpolation of the relationship for 1995 and 2004.

Figures 2b and 2d show the derived relationships of ice age and thickness for April and September from 1984 to 2018. After the annual cycle of the relationship between ice age and thickness is linearly interpolated to the weekly scale, we convert weekly ice age to weekly ice thickness and determine the daily ice thickness using linear interpolation and thus calculate the monthly mean ice thickness. An example of such conversion is shown in Figure 4.

Monthly mean ice thickness in the 12.5 km EASE-Grid is then remapped to 25 km polar stereographic projection to match the spatial resolution of sea ice concentration. The PIOMAS and OTIM monthly mean ice thickness are also remapped to the same polar projection. Monthly mean Arctic sea ice volume is calculated as the product of sea ice thickness, ice concentration, and grid cell area of all grid cells over an area defined in RK18. Bounded by the gateways into the Pacific (Bering Strait), the Canadian Arctic Archipelago, and the Greenland (Fram Strait) and Barents Seas, the area covers approximately 7.23×10^6 km^2. We will refer to this area as the Arctic Ocean, as in RK18. Monthly mean sea ice thickness is also calculated over the DRA, as defined in RPW08. Hereinafter, we call the sea ice thickness and sea ice volume derived from the ice age product as "IceAgeDerived."

3 Results

3.1 Evaluation of ice thickness and Arctic ice volume

Based on submarine sonar data, RPW08 derived an equation – Eq. 9 in their paper and Eq. 2 here – to calculate the inter-annually averaged ice thickness over the DRA with the annual cycle superimposed. Mean sea ice thickness over the DRA in February and March, as well as in October and November, from 1984 to 2000 are calculated here using this equation. RK18 reported the mean sea ice thickness over the DRA from ICESat in February and March 2004-2008, and in October and November 2003-2007, and from CryoSat-2 in February and March and in October and November 2011-2018. RK18 also reported monthly mean Arctic ice volume over the Arctic Ocean from ICESat in February and March 2004-2008 and in October and November 2003-2007, and from CryoSat-2 in February and March and in October and November 2011-2018. These data are used to evaluate the quality of sea ice thickness and volume of the IceAgeDerived.

IceAgeDerived sea ice thickness over the DRA is close to the one-to-one line in comparison to ice thickness from submarine in February/March, with a bias of 0.03 m, RMSE of 0.074 m, and R-squared value of 0.96 (Figure 5 and Table 1). In October/November the bias is -0.035 m, the RMSE is 0.14 m, and the R-squared is 0.97. Compared to ICESat, sea ice thickness over the DRA gives a slightly larger bias and RMSE and slightly smaller R-squared, with a bias of -0.014 m, RMSE of 0.096 m, and R-squared of 0.75 in February/March (Figure 5, Table 1). In October/November, the bias is 0.20 m, the RMSE is 0.16 m, and the R-squared is 0.93. The bias and RMSE values are well within the uncertainty of ICESat ice

https://doi.org/10.5194/tc-2019-192
Preprint. Discussion started: 26 August 2019

thickness estimates of 0.37 m (Kwok and Rothrock, 2009). Comparison to CryoSat-2 sea ice thickness over DRA shows a bias of -0.21 m and RMSE of 0.079 m for February/March, and a bias of -0.04 m and RMSE of 0.14 m for October/November. These are comparable in magnitude to those from ICESat, and within the uncertainty of CryoSat-2 ice thickness (Kwok 2018). The R-squared in October/November is close to 0, which indicates the IceAgeDerived sea ice thickness has similar values, but does not follow the changes in CryoSat-2 sea ice thickness in October/November from 2011 to 2018 (Figure 5 and Table 1). Comparing the results of PIOMAS to submarine and ICESat thickness in Table 1 show similar bias and RMSE results as those in Schweiger et al. (2011).

Measurements of IceAgeDerived sea ice volume over the Arctic Ocean agree with those from ICESat in February/March, with a bias of -0.72×10^3 km^3, RMSE of 0.74×10^3 km^3, and R-squared of 0.87 (Figure 6 and Table 2). In October/November, IceAgeDerived sea ice volume is largely underestimated compared to ICESat, with a bias of -3.95×10^3 km^3, even though IceAgeDerived sea ice thickness measurements agree well with those from ICESat over DRA. Similar underestimations in October/November are found for PIOMAS and OTIM when compared to ICESat. Comparison to CryoSat-2 sea ice volume shows low bias and low RMSE, where the bias is 0.29×10^3 km^3 (-0.66×10^3 km^3) and the RMSE is 0.75×10^3 km^3 (0.98×10^3 km^3) in February/March (October/November).

Comparisons of sea ice thickness over DRA and sea ice volume over the Arctic Ocean from PIOMAS and OTIM to submarine ULS, ICESat and CryoSat-2 are also shown in Figures 5 and 6, and in Tables 1 and 2. IceAgeDerived products show comparable or slightly better results in terms of bias, RMSE, and R-squared. The better agreement with submarine ULS can be attributed to the fact that the IceAgeDerived product is developed based on matched ice age and submarine ULS ice thickness data. However, it should be noted that while submarine data in April and September are used in the algorithm development, the comparisons are in February/March and October/November.

3.2 Sea ice thickness and volume climatology and trend

The spatial distributions of the ice thickness over the Arctic from 1984 to 2018 show similar spatial patterns, but different magnitudes in the four seasons (Figure 7). Sea ice is thickest along the northern portion of the Canadian Archipelago and Greenland, decreasing radially, with the thinnest ice over the Arctic's peripheral seas on the Eurasia side. The thickest sea ice appears in the spring, around 3 m in the Canada Basin and North Pole areas. The thinnest sea ice is in early fall, around or less than 1 m over the coastal areas of the Kara, Laptev, and Chukchi Seas. The spatial distributions of PIOMAS and OTIM (Figures A1 and A2 in the Appendix) show similar patterns, while the ice thickness north of the Canadian Archipelago and Greenland is thinner, especially when compared to PIOMAS.

The annual cycle of monthly mean sea ice volume over the Arctic Ocean shows a minimum value in September at around 6770 km^3, then increasing to the maximum value in the following May at around 21737 km^3, followed by a decrease. This annual cycle is certainly affected by the theoretical model used to depict the ice growth/melt as shown in Figure 3. The annual cycle closely follows the sea ice volume annual cycle of the PIOMAS (Figure 8), which uses a different approach to derive ice thickness and ice volume. The IceAgeDerived exhibits its largest sea ice volume difference of 2004 km^3 in May.

https://doi.org/10.5194/tc-2019-192
Preprint. Discussion started: 26 August 2019

This difference can be attributed to the relatively thicker sea ice from the IceAgeDerived in the years before 2000, which is discussed further below. Ice volume over the Arctic Ocean from OTIM has a similar annual cycle but with a larger magnitude, with the maximum in April and the minimum in September.

The time series of sea ice thickness over DRA in February and March from 1984 to 2018 shows a decreasing trend from 1984 to 2000 and close agreement with the time series from submarine ULS, a generally decreasing trend from 2004 to 2008 as also shown in time series from ICESat, and a relatively unchanging state from 2011 to 2018 as also depicted in time series from CryoSat-2 (Figure 9a). A similar conclusion can be drawn for the time series in October and November (Figure 9b). The overall decreasing trends are consistent with observations of the replacement of multiyear sea ice with first year ice in the Arctic Ocean, and partial recovery of multiyear sea ice after the summer of 2008 (Maslanik et al. 2007, Maslanik et al. 2011). Compared to the PIOMAS ice thickness, in February/March the sea ice thickness in the 1980s is mostly greater, and remains close to or smaller than that of PIOMAS from 2004 to 2008, and is smaller from 2011 to 2018. In October/November the sea ice thickness is greater in the 1980s, comparable from 1990 to 2010, and then larger afterwards. OTIM shows smaller ice thicknesses than both IceAgeDerived and PIOMAS in October/November, and mostly larger ice thickness in February/March except in the 1980s.

The similarities and differences found here are consistent with the results shown in Figure 5 and Table 1, and partly explain the differences in the sea ice volume annual cycles shown in Figure 8. The time series of PIOMAS, and their comparisons with ICESat shown here, are similar to those in Schweiger et al. (2011). As a result of the differences in ice thickness from 1984 to 2018, the overall trends of ice thickness over the DRA from 1984 to 2018 are -0.054, -0.035, and -0.036 m/year in February/March, and -0.040, -0.042, and -0.026 m/year in October/November for IceAgeDerived, PIOMAS, and OTIM respectively, with significance levels all higher than 95%.

Time series of sea ice volume over the Arctic Ocean show generally decreasing trends from 1984 to around 2008, and relatively stable conditions from 2011 to 2018 both in February/March and October/November, similar to the time series from PIOMAS and OTIM (Figure 10). This overall decrease agrees well with the dramatic decrease in sea ice extent and disappearance of multiyear sea ice reported in the literature (Stroeve et al. 2012, Maslanik et al. 2007, Maslanik et al. 2011). In February/March, PIOMAS shows smaller ice volume from 1984 to 2000 and similar values after 2000; OTIM shows higher ice volume after the 1990s. In October/November, PIOMAS shows smaller values in the 1980s and similar values afterwards, while OTIM shows consistently smaller ice volume before 2000. All three sea ice volumes are much lower than those from ICESat for 2003 to 2007 with comparable sea ice thickness over the DRA in those years; all three sea ice volumes are comparable to that from CryoSat-2, with similar results for sea ice thickness over the DRA. All these findings are consistent with what is shown in Figure 6 and Table 2. As with the results of the differences in ice volumes from 1984 to 2018, the overall trends in ice volume over the Arctic Ocean from 1984 to 2018 are -474, -258, and -311 km^3/year in February/March, and -342, -305, and -230 km^3/year in October/November for IceAgeDerived, PIOMAS, and OTIM respectively, with significance levels all higher than 95%. IceAgeDerived shows stronger ice volume reduction over the Arctic Ocean in February/March and in October/November when compared to PIOMAS and OTIM.

https://doi.org/10.5194/tc-2019-192
Preprint. Discussion started: 26 August 2019

Arctic sea ice volume over the Arctic Ocean from 1984 to 2018 has been decreasing in every month of the year (Figure 11). The most volume reductions from December to June occur from the 1990s to the 2000s and from the 2000s to 2010s. From July to November, the volume reductions from the 1980s to 1990s are comparable to those from the 1990s to 2000s. The volume reductions in all months are the least from the 2000s to the 2010s. It should be noted that the data in the 1980s starts in 1984, and the data for the 2010s ends in 2018. Though the decadal mean annual cycles of sea ice volume are similar in shape, the magnitudes of the cycles - in terms of the difference between April and September - have been decreasing, with around 18871 km^3 in the 1980s and 12169 km^3 in the 2010s.

Time series of the monthly mean sea ice volume over the Arctic Ocean for all months from 1984 to 2018 have similar features to those in February/March and October/November, with higher values in the 1980s than those of PIOMAS and OTIM, a generally decreasing trend from 1984 to 2008 as with PIOMAS and OTIM, and relatively stable conditions from 2011 to 2018, similar to PIOMAS and OTIM (Figure 12). As a result, the sea ice volume trends from the IceAgeDerived in every month are higher than those from PIOMAS and OTIM, except being comparable to PIOMAS from August to October (Figure 13). The monthly trends exhibit an annual cycle, with the maximum magnitude in May at -537 km^3/year and minimum magnitude in September of -251 km^3/year, which is the opposite of the annual cycle trend of mean sea ice thickness. OTIM also exhibits this feature, while the annual cycle of volume trends from PIOMAS shows no apparent monthly differences. The mean monthly trend of all months over the Arctic Ocean from 1984 to 2018 is -411 km^3/year, which is higher in magnitude compared to -282 km^3/year from PIOMAS and -269 km^3/year from OTIM, with significance levels all higher than 95%. The PIOMAS mean monthly trend is similar to that derived from PIOMAS sea ice volume data for 1979 to 2012, -2.8×103 km^3/decade with an uncertainty of 1.0×103 km^3/decade as shown in Schweiger et al. (2011). The IceAgeDerived ice volume shows a stronger reduction in ice volume over the Arctic Ocean from 1984 to 2018.

Causes for the changes in the Arctic sea ice volume can be partitioned roughly into two categories: changes from sea ice thickness and changes from sea ice area. In a manner similar to that used by Liu et al. (2009), this partitioning can be estimated by:

$$\frac{dV}{dt} = \frac{d(\sum A_i H_i)}{dt} \cong \frac{d(\bar{A}\bar{H})}{dt} = \bar{A}\frac{d\bar{H}}{dt} + \bar{H}\frac{d\bar{A}}{dt} \quad (7)$$

where V is the sea ice volume over the Arctic Ocean, A_i and H_i are the sea ice area and thickness in individual grid cells over the Arctic Ocean, and $\bar{A}$ and $\bar{H}$ are the mean sea ice area and thickness over the Arctic Ocean. The term $\bar{A}(d\bar{H}/dt)$ represents the contribution of sea ice thickness changes to the overall trend, and the term $\bar{H}(d\bar{A}/dt)$ represents the contribution of the sea ice area changes. For the Arctic sea ice volume from 1984 to 2018, the changes in sea ice thickness contribute to approximately 80% or more of the total trends from November to May; these contributions decrease to around 50% in August and September. The changes in sea ice area contribute to less than 30% of total trends in all months, with even lower contributions from December to May, which are less than 10%. PIOMAS shows similar trends, while OTIM shows a greater contribution from the sea ice area changes and less contribution of sea ice thickness changes from June to October. It should

https://doi.org/10.5194/tc-2019-192
Preprint. Discussion started: 26 August 2019

be noted that the sum of these two contributions is not 100% because of the use of the production of area means of thickness and ice area to approximately represent the total ice volume.

4 Discussion and Conclusions

In this study, a multi-decadal Arctic sea ice thickness dataset covering the period 1984 to 2018 is created from an existing satellite-derived ice age product. The relationship between ice age and ice thickness is first established based on submarine upward-looking sonar ice draft observations from 1984 to 2000, and ICESat ice thickness from 2003 to 2008. Both are available for only two calendar months. Therefore, an empirical model of the annual cycle of sea ice thickness growth is used to derive the ice age and ice thickness relationship for every month from 1984 to 2018. Sea ice volume over the Arctic Ocean is then calculated from ice thickness and concentration. Comparisons of the time series of derived ice thickness and ice volume with those from the literature and other data sets using different approaches show general similarities but with some notable differences. The agreement proves the soundness of the ice aged-based ice thickness and ice volume dataset, while the differences indicate there is room for further improvement in all the ice thickness data sets.

The major findings of this study include:

- Sea ice thickness derived from ice age ("IceAgeDerived") over the DRA (the submarine data release area) shows good agreement with ice thickness from submarine ULS, ICESat, and CryoSat-2 in both February/March and October/November, with low bias and RMSE and a high R-squared, except for a near-zero R-squared with CryoSat-2 in October/November. IceAgeDerived sea ice volume over the Arctic Ocean shows good agreement with that from ICESat and CryoSat-2. Compared to ICESat, it has a low bias and RMSE and a high R-squared in February/March. In October/November it has a high negative bias, low RMSE, and high R-squared. Compared to CryoSat-2, it has low bias, RMSE, and R-squared values in both February/March and October/November.
- Sea ice is thickest north of the Canadian Archipelago and Greenland, decreasing radially, with the thinnest ice over the Arctic's peripheral seas on the Eurasia side of the Arctic Ocean. Sea ice volume over the Arctic Ocean has its minimum value in September, increasing to a maximum value in the following May.
- In both February/March and October/November, the time series of sea ice thickness over DRA from the IceAgeDerived shows a decreasing trend from 1984 to 2000, as does the submarine ULS data, a generally decreasing trend from 2003 to 2008 similar to that of ICESat, and a relatively stable state from 2011 to 2018 like the CryoSat-2 ice thickness.
- Sea ice volume over the Arctic Ocean shows a generally decreasing trend from 1984 to around 2008, and relatively stable conditions afterwards in almost every month. The mean monthly trend of all months from 1984 to 2018 is -411 km^3/year, which shows a stronger ice volume reduction than PIOMAS (-282

https://doi.org/10.5194/tc-2019-192
Preprint. Discussion started: 26 August 2019

km^3/year) and OTIM (-269 km^3/year). This difference can be attributed to the higher sea ice volume over the Arctic Ocean from the IceAgeDerived in the 1980s.

- Changes in sea ice thickness contribute 80% or more to the sea ice volume trend from 1984 to 2018 from November to May, decreasing to a contribution of about 50% in August and September. The changes in sea ice area contribute less than 30% to the trends in all months, with even lower contributions from November to May.

Although the ice thickness and volume dataset presented here is a consistent and accurate multidecadal product, there are some areas for potential improvement. First, a linear relationship between ice age and ice thickness is assumed, which may not be strictly valid. Of particular interest is the observation that submarine data shows a slightly thinner ice thickness for ice more than four years old than that for four-year old ice, though ICESat shows the same in only one year. To determine whether this relationship is valid, other collocated ice age and ice thickness data, e.g. from the recently launched ICESat-2 (Markus et al. 2017) should be analyzed. Second, the annual cycle of ice thickness growth/decline is assumed to be linear from September to the following May and from May to September, which also may not be valid. RPW08 conceptualized sea ice growth and decline as a sine function. A more sophisticated model of the annual cycle of sea ice growth/decline may be needed in deriving the ice age and ice thickness relationship. The annual cycle of trends in ice volume over the Arctic Ocean appears to be opposite to the annual cycle of ice growth. This requires further investigation. Third, in deriving the relation of ice age to ice thickness in the years before 2000, only ice draft measurements from submarine ULS over the DRA, e.g. over or near the central Arctic Ocean, are available. The derived relationship may be skewed to higher ice thicknesses. Thus, Arctic ice volume derived in this study before 2004 might be overestimated. Correcting this relationship requires more spatially representative ice thickness measurements, or a well-designed parameterization scheme.

Future improvements in ice thickness estimation may require work on 1) improving our understanding and parameterization of the forcing and physical processes controlling the ice growth and melt, 2) reducing uncertainties in the ancillary data required for ice thickness estimation, 3) collecting extensive temporally and spatially representative ice thickness measurements for better evaluation, 4) designing new models or approaches to estimate ice thickness.

Snow depth over the sea ice is one of the key parameters in the sea ice thickness retrieval for all existing satellite data sets. Though progress has been made in reducing the uncertainties in estimating snow depth from space, its uncertainty remains high (Lawrence et al. 2018, Shalina et al. 2018). One major challenge for improving sea ice thickness retrievals is the lack of "truth" validation data sets. Because of the severe environmental conditions in the polar regions, in situ ice thickness measurements are scarce, which limits our ability to identify the issues in current data sets and to make further improvement. Ice thickness products using new approaches may provide additional evaluation of existing products. A better overall product benefits from all the above-mentioned efforts, and may come as an ensemble of multiple ice thickness products if we know the limitations and strengths of each data set.

https://doi.org/10.5194/tc-2019-192
Preprint. Discussion started: 26 August 2019

5 Code availability

Code in Interactive Data Language (IDL) to process the input data, to generate the data sets, and to analyze the data sets is available upon request from Y.L.

6 Data availability

Data used to generate the ice thickness and ice volume data sets are available from the National Snow and Ice Data Center (NSIDC) as detailed in the manuscript. The derived ice thickness and ice volume data sets are available upon request from Y.L.

7 Author contributions

Y.L. and J.K. conceived the idea of this study. Y.L. analysed the data and generated the ice thickness and ice volume data sets, analysed the results, and wrote the manuscript with contributions from all the co-authors. J.K. provided valuable guidance on the work and editing of the manuscript. X.W. provided and advised on the usage of the OTIM ice thickness. M.T. advised on the usage of the ice age data. All authors assisted in writing and editing the manuscript.

8 Competing interests

The authors declare that they have no competing interests.

9 Acknowledgments

This work was supported by the NOAA National Climatic Data Center (NCDC) and the Joint Polar Satellite System (JPSS) Program Office. Y.L. would like to thank Ms. Leanne Avila for editing the manuscript. The views, opinions, and findings contained in this report are those of the author(s) and should not be construed as an official National Oceanic and Atmospheric Administration or U.S. Government position, policy, or decision.

References

Aman, A. A. and Bman, B. B.: The test article, J. Sci. Res., 12, 135–147, doi:10.1234/56789, 2015.

Aman, A. A., Cman, C., and Bman, B. B.: More test articles, J. Adv. Res., 35, 13–28, doi:10.2345/67890, 2014.

Cavalieri, D. J., C. L. Parkinson, P. Gloersen, and H. J. Zwally.: updated yearly. Sea Ice Concentrations from Nimbus-7 SMMR and DMSP SSM/I-SSMIS Passive Microwave Data, Version 1. Boulder, Colorado USA. NASA National Snow and

https://doi.org/10.5194/tc-2019-192
Preprint. Discussion started: 26 August 2019

Ice Data Center Distributed Active Archive Center. doi: https://doi.org/10.5067/8GQ8LZQVL0VL. [Date Accessed in January 2019], 1996.

Gregory, J. M., Stott, P. A., Cresswell, D. J., Rayner, N. A., Gordon, C., and Sexton, D. M. H.: Recent and future changes in Arctic sea ice simulated by the HadCM3 AOGCM, Geophysical Research Letters, 29, 28-21, 2002.

Ivanova, N., Pedersen, L. T., Tonboe, R. T., Kern, S., Heygster, G., Lavergne, T., Sørensen, A., Saldo, R., Dybkjær, G., and Brucker, L.: Inter-comparison and evaluation of sea ice algorithms: towards further identification of challenges and optimal approach using passive microwave observations, The Cryosphere, 9, 1797-1817, 2015.

Key, J., Wang, X., Liu, Y., Dworak, R., and Letterly, A.: The AVHRR Polar Pathfinder Climate Data Records, Remote Sensing, 8, 167, 2016.

Kurtz, N. T., Galin, N., and Studinger, M.: An improved CryoSat-2 sea ice freeboard retrieval algorithm through the use of waveform fitting, The Cryosphere, 8, 1217-1237, 2014.

Kwok, R., and Cunningham, G. F.: ICESat over Arctic sea ice: Estimation of snow depth and ice thickness, Journal of Geophysical Research: Oceans, 113, 2008.

Kwok, R., and Rothrock, D. A.: Decline in Arctic sea ice thickness from submarine and ICESat records: 1958–2008, Geophysical Research Letters, 36, 2009.

Kwok, R.: Arctic sea ice thickness, volume, and multiyear ice coverage: losses and coupled variability (1958–2018), Environmental Research Letters, 13, 105005, 2018.

Lawrence, I. R., Tsamados, M. C., Stroeve, J. C., Armitage, T. W. K., and Ridout, A. L.: Estimating snow depth over Arctic sea ice from calibrated dual-frequency radar freeboards, The Cryosphere, 12, 3551-3564, 2018.

Laxon, S. W., Giles, K. A., Ridout, A. L., Wingham, D. J., Willatt, R., Cullen, R., Kwok, R., Schweiger, A., Zhang, J., and Haas, C.: CryoSat-2 estimates of Arctic sea ice thickness and volume, Geophysical Research Letters, 40, 732-737, 2013.

Letterly, A., Key, J., and Liu, Y.: Arctic climate: changes in sea ice extent outweigh changes in snow cover, The Cryosphere, 12, 3373-3382, 2018.

Lindsay, R., Haas, C., Hendricks, S., Hunkeler, P., Kurtz, N., Paden, J., Panzer, B., Sonntag, J., Yungel, J., and Zhang, J.: Seasonal forecasts of Arctic sea ice initialized with observations of ice thickness, Geophysical research letters, 39, 2012.

Liu, Y., Key, J., and Wang, X.: Influence of changes in sea ice concentration and cloud cover on recent Arctic surface temperature trends, Geophysical Research Letters, 36, 10.1029/2009GL040708, 2009.

Liu, Y., Key, J., and Mahoney, R.: Sea and Freshwater Ice Concentration from VIIRS on Suomi NPP and the Future JPSS Satellites, Remote Sensing, 8, 523, 2016.

Markus, T., Neumann, T., Martino, A., Abdalati, W., Brunt, K., Csatho, B., Farrell, S., Fricker, H., Gardner, A., and Harding, D.: The Ice, Cloud, and land Elevation Satellite-2 (ICESat-2): science requirements, concept, and implementation, Remote sensing of environment, 190, 260-273, 2017.

Maslanik, J., Stroeve, J., Fowler, C., and Emery, W.: Distribution and trends in Arctic sea ice age through spring 2011, Geophysical Research Letters, 38, 2011.

https://doi.org/10.5194/tc-2019-192
Preprint. Discussion started: 26 August 2019

Maslanik, J. A., Fowler, C., Stroeve, J., Drobot, S., Zwally, J., Yi, D., and Emery, W.: A younger, thinner Arctic ice cover: Increased potential for rapid, extensive sea-ice loss, Geophysical Research Letters, 34, 2007.

National Snow and Ice Data Center (comp.). updated 2006. Submarine Upward Looking Sonar Ice Draft Profile Data and Statistics, Version 1. [Indicate subset used]. Boulder, Colorado USA. NSIDC: National Snow and Ice Data Center. doi: https://doi.org/10.7265/N54Q7RWK. [Date Accessed January 2019], 1998.

Perovich, D. K., Nghiem, S. V., Markus, T., and Schweiger, A.: Seasonal evolution and interannual variability of the local solar energy absorbed by the Arctic sea ice–ocean system, Journal of Geophysical Research: Oceans, 112, 2007.

Pistone, K., Eisenman, I., and Ramanathan, V.: Observational determination of albedo decrease caused by vanishing Arctic sea ice, Proceedings of the National Academy of Sciences, 111, 3322-3326, 2014.

Rothrock, D. A., Yu, Y., and Maykut, G. A.: Thinning of the Arctic sea-ice cover, Geophysical Research Letters, 26, 3469-3472, 1999.

Rothrock, D. A., and Wensnahan, M.: The accuracy of sea ice drafts measured from US Navy submarines, Journal of Atmospheric and Oceanic Technology, 24, 1936-1949, 2007.

Rothrock, D. A., Percival, D. B., and Wensnahan, M.: The decline in arctic sea-ice thickness: Separating the spatial, annual, and interannual variability in a quarter century of submarine data, Journal of Geophysical Research: Oceans, 113, 2008.

Schweiger, A. J., Wood, K. R., and Zhang, J.: Arctic sea ice volume variability over 1901–2010: A model-based reconstruction, Journal of Climate, 32, 4731-4752, 2019.

Schweiger, A., Lindsay, R., Zhang, J., Steele, M., Stern, H., and Kwok, R.: Uncertainty in modeled Arctic sea ice volume, Journal of Geophysical Research: Oceans, 116, 2011.

Screen, J. A., and Simmonds, I.: The central role of diminishing sea ice in recent Arctic temperature amplification, Nature, 464, 1334, 2010.

Shalina, E. V., and Sandven, S.: Snow depth on Arctic sea ice from historical in situ data, The Cryosphere, 12, 1867-1886, 2018.

Stroeve, J., Holland, M. M., Meier, W., Scambos, T., and Serreze, M.: Arctic sea ice decline: Faster than forecast, Geophysical research letters, 34, 2007.

Stroeve, J., Barrett, A., Serreze, M., and Schweiger, A.: Using records from submarine, aircraft and satellites to evaluate climate model simulations of Arctic sea ice thickness, Cryosphere, 8, 2014.

Stroeve, J. C., Serreze, M. C., Holland, M. M., Kay, J. E., Malanik, J., and Barrett, A. P.: The Arctic's rapidly shrinking sea ice cover: a research synthesis, Climatic Change, 110, 1005-1027, 2012.

Sévellec, F., Fedorov, A. V., and Liu, W.: Arctic sea-ice decline weakens the Atlantic meridional overturning circulation, Nature Climate Change, 7, 604, 2017.

Tian-Kunze, X., Kaleschke, L., Maaß, N., Mäkynen, M., Serra, N., Drusch, M., and Krumpen, T.: SMOS-derived thin sea ice thickness: algorithm baseline, product specifications and initial verification, The Cryosphere, 8, 997-1018, 2014.

https://doi.org/10.5194/tc-2019-192
Preprint. Discussion started: 26 August 2019

Tschudi, M., Stroeve, J., and Stewart, J.: Relating the age of Arctic sea ice to its thickness, as measured during NASA's ICESat and IceBridge campaigns, Remote Sensing, 8, 457, 2016.

Tschudi, M. A., Meier, W. N., and Stewart, J. S.: An enhancement of sea ice motion and age products, The Cryosphere Discussion, 2019.

485 Tschudi, M., W. N. Meier, J. S. Stewart, C. Fowler, and J. Maslanik. 2019. *EASE-Grid Sea Ice Age, Version 4*. Boulder, Colorado USA. NASA National Snow and Ice Data Center Distributed Active Archive Center. doi: https://doi.org/10.5067/UTAV7490FEPB. [Data Acessed in May 2019], 2019.

Wang, X., Key, J. R., and Liu, Y.: A thermodynamic model for estimating sea and lake ice thickness with optical satellite data, Journal of Geophysical Research: Oceans, 115, 2010.

490 Wang, X., Key, J., Kwok, R., and Zhang, J.: Comparison of Arctic sea ice thickness from satellites, aircraft, and PIOMAS data, Remote Sensing, 8, 713, 2016.

Zhang, J., and Rothrock, D. A.: Modeling global sea ice with a thickness and enthalpy distribution model in generalized curvilinear coordinates, Monthly Weather Review, 131, 845-861, 2003.

https://doi.org/10.5194/tc-2019-192
Preprint. Discussion started: 26 August 2019

495

Table 1: Statistics of comparison of ice thickness over the SCIEX box from IceAgeDerived, PIOMAS, and OTIM and from submarine up-looking sonar 1984-2000, ICESat 2004-2008, and Cryosat-2 2011-2018 in February/March (top row), and October/November (bottom row).

Ice thickness		Submarine up-looking sonar 1984-2000 Feb/Mar (Oct/Nov)	ICESat 2004-2008 Feb/Mar (Oct/Nov)	Cryosat-2 2011-2018 Feb/Mar (Oct/Nov)
IceAgeDerived	Bias (m)	0.03 -0.035	-0.014 0.20	-0.21 -0.04
	RMSE (m)	0.074 0.14	0.096 0.16	0.079 0.14
PIOMAS	Bias (m)	-0.16 -0.055	0.12 0.14	-0.10 -0.24
	RMSE (m)	0.31 0.30	0.16 0.097	0.13 0.16
OTIM	Bias (m)	0.16 -0.60	0.49 -0.13	0.21 -0.37
	RMSE (m)	0.26 0.28	0.16 0.22	0.21 0.22

500

https://doi.org/10.5194/tc-2019-192
Preprint. Discussion started: 26 August 2019

The Cryosphere Discussions
Open Access
EGU

Table 2: Statistics of comparison of Arctic ice volume from IceAgeDerived, PIOMAS, and OTIM and from ICESat 2004-2008, and Cryosat-2 2011-2018 in February/March (top row), and October/November (bottom row).

Ice thickness		ICESat 2004-2008 Feb/Mar (Oct/Nov)	Cryosat-2 2011-2018 Feb/Mar (Oct/Nov)
IceAgeDerived	Bias (10^3 km^3)	-0.72 -3.95	0.29 -0.66
	RMSE (10^3 km^3)	0.74 0.76	0.75 0.98
PIOMAS	Bias (10^3 km^3)	0.44 -4.21	0.90 -1.70
	RMSE (10^3 km^3)	0.98 0.68	0.96 0.98
OTIM	Bias (10^3 km^3)	4.20 -4.86	3.87 -1.63
	RMSE (10^3 km^3)	1.20 0.96	1.48 1.23

505

https://doi.org/10.5194/tc-2019-192
Preprint. Discussion started: 26 August 2019

The Cryosphere
Discussions
Open Access
EGU

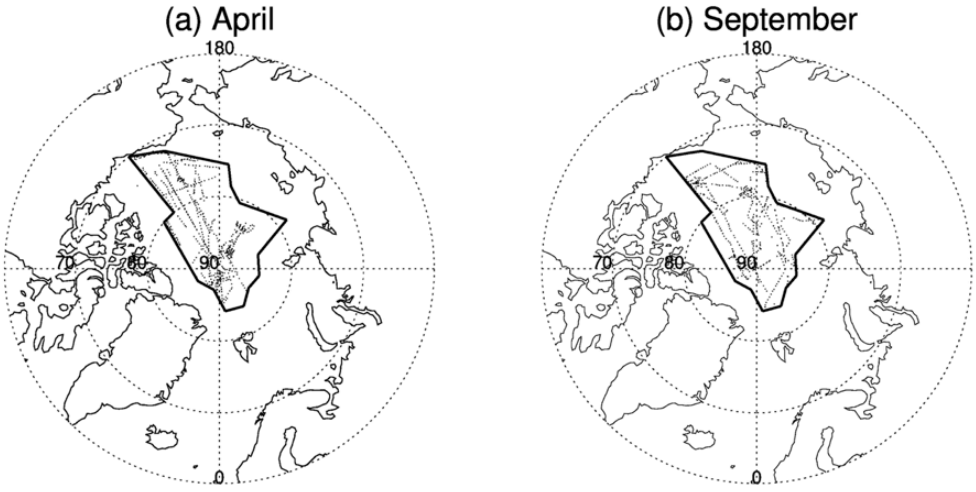

Figure 1: U.S. submarine sea ice draft observations in April (a) and September (b) over the Arctic Ocean from 1984 to 2000.

https://doi.org/10.5194/tc-2019-192
Preprint. Discussion started: 26 August 2019

510

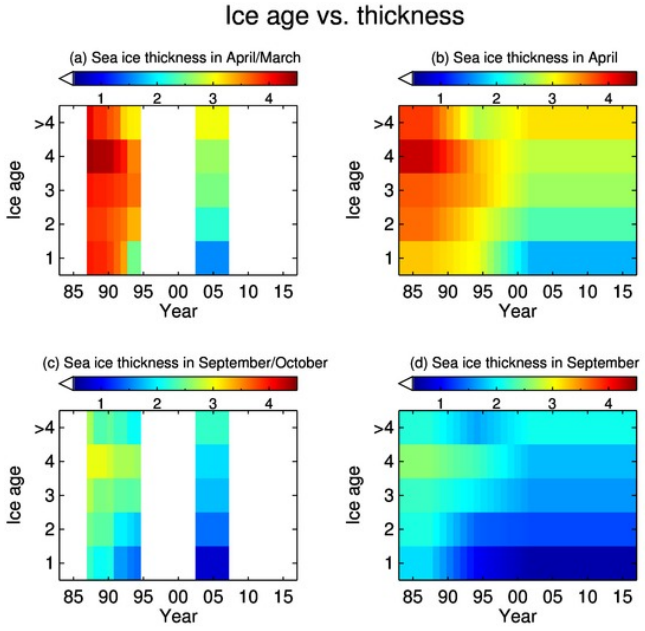

Figure 2: Observed relationship of ice age and ice thickness from 1988 to1995 from submarine data in April (a) and September (c), and from 2004 to 2008 from ICESat in March (a) and October (c), and derived relationship of ice age and ice thickness from 1984 to 2018 in April (b) and September (d).

515

https://doi.org/10.5194/tc-2019-192
Preprint. Discussion started: 26 August 2019

The Cryosphere
Discussions
Open Access
EGU

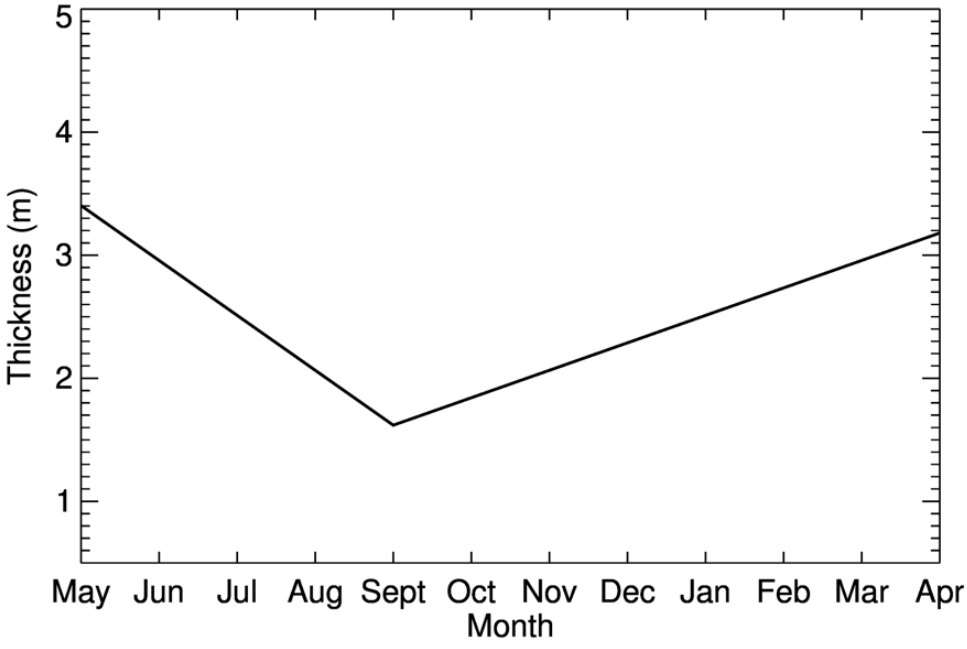

Figure 3: Annual cycle of sea ice thickness.

https://doi.org/10.5194/tc-2019-192
Preprint. Discussion started: 26 August 2019

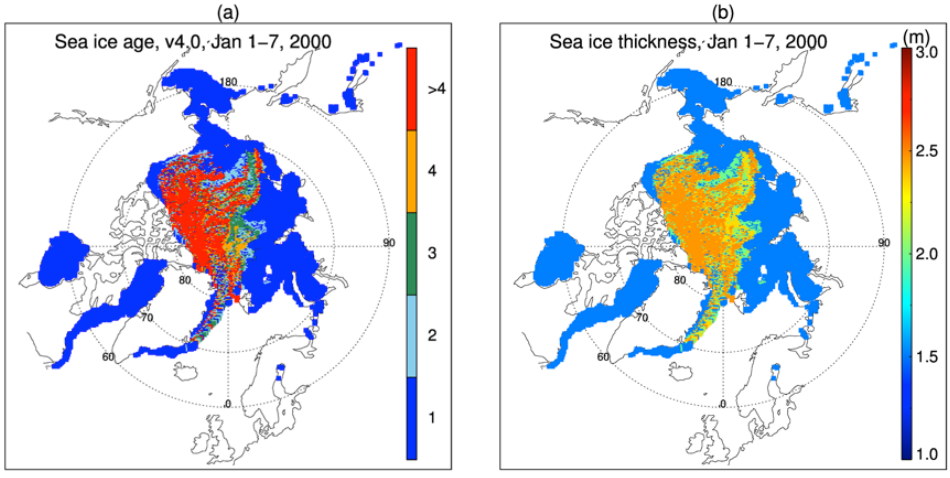

Figure 4: Ice age and ice thickness derived from ice age from January 1 to 7, 2000.

https://doi.org/10.5194/tc-2019-192
Preprint. Discussion started: 26 August 2019

The Cryosphere
Discussions
Open Access
EGU

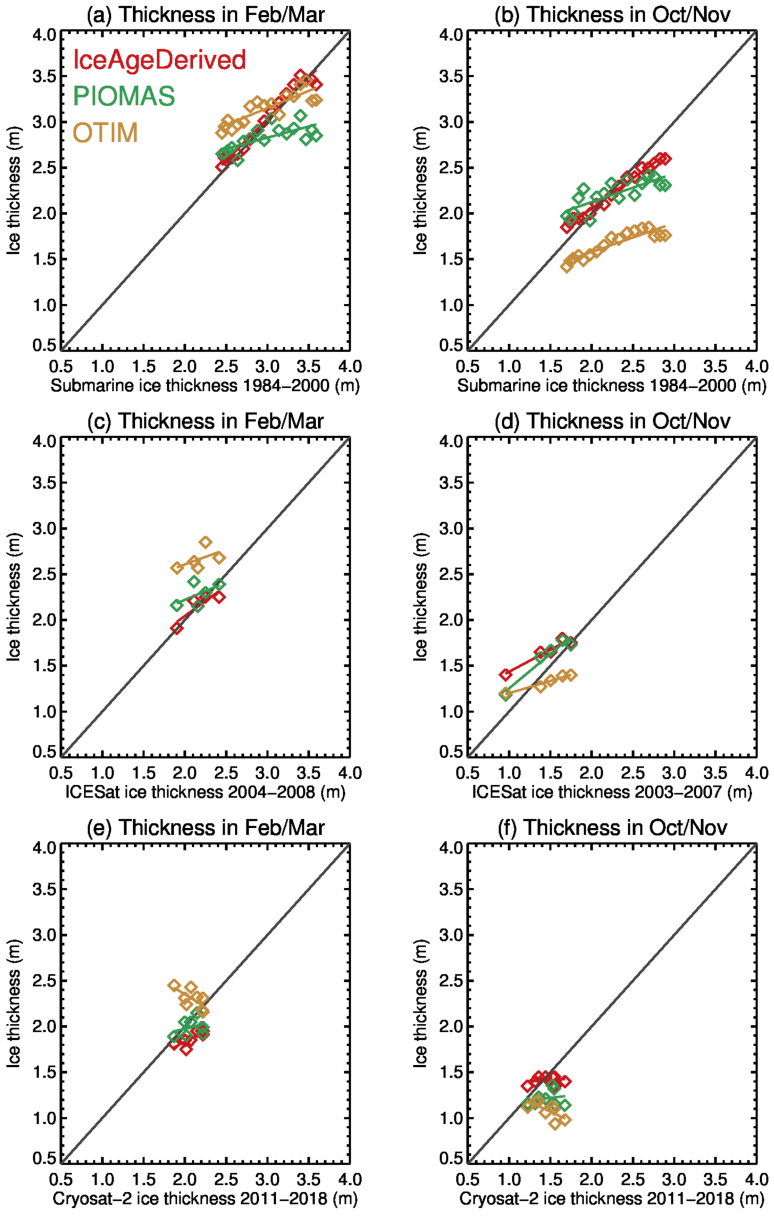

Figure 5: Comparison of ice thickness over the SCIEX box from IceAgeDerived, PIOMAS, and OTIM and from submarine up-looking sonar 1984-2000, ICESat 2004-2008, and Cryosat-2 2011-2018.

https://doi.org/10.5194/tc-2019-192
Preprint. Discussion started: 26 August 2019

The Cryosphere
Discussions
Open Access
EGU

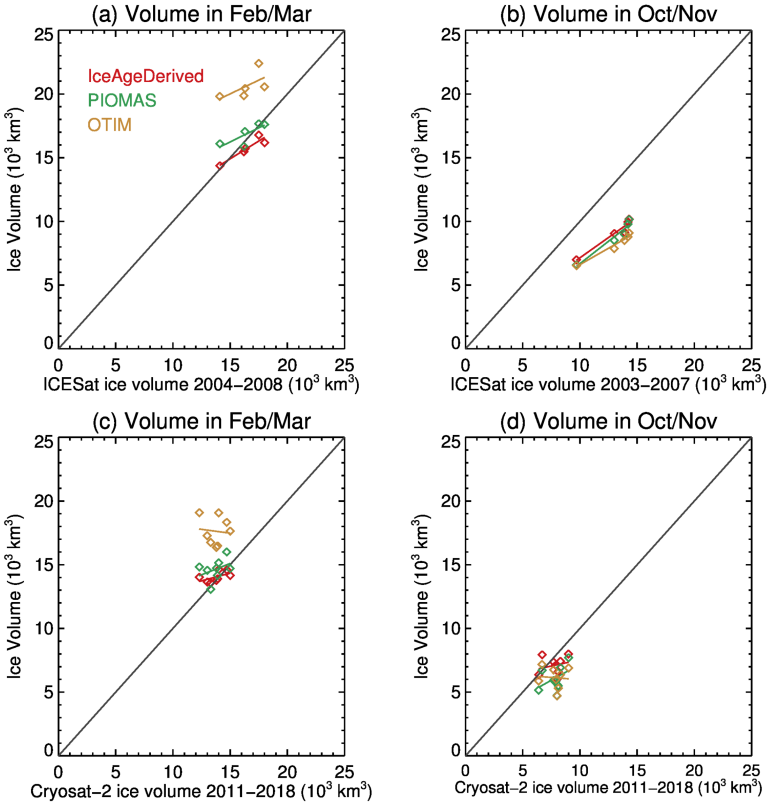

Figure 6: Comparison of ice thickness over the SCIEX box from IceAgeDerived, PIOMAS, and OTIM and from ICESat 2004-2008, and Cryosat-2 2011-2018.

530

https://doi.org/10.5194/tc-2019-192
Preprint. Discussion started: 26 August 2019

The Cryosphere
Discussions
Open Access
EGU

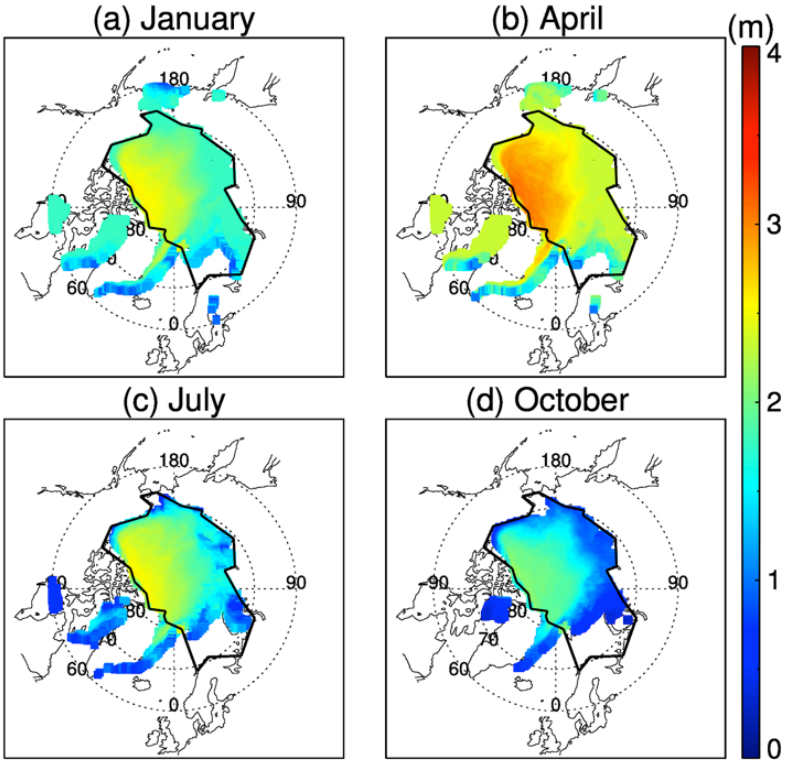

Figure 7: Derived climatological mean sea ice thickness distribution 1984 to 2018 from ice age in the Arctic in January, April, July, and October.

https://doi.org/10.5194/tc-2019-192
Preprint. Discussion started: 26 August 2019

The Cryosphere
Discussions
Open Access
EGU

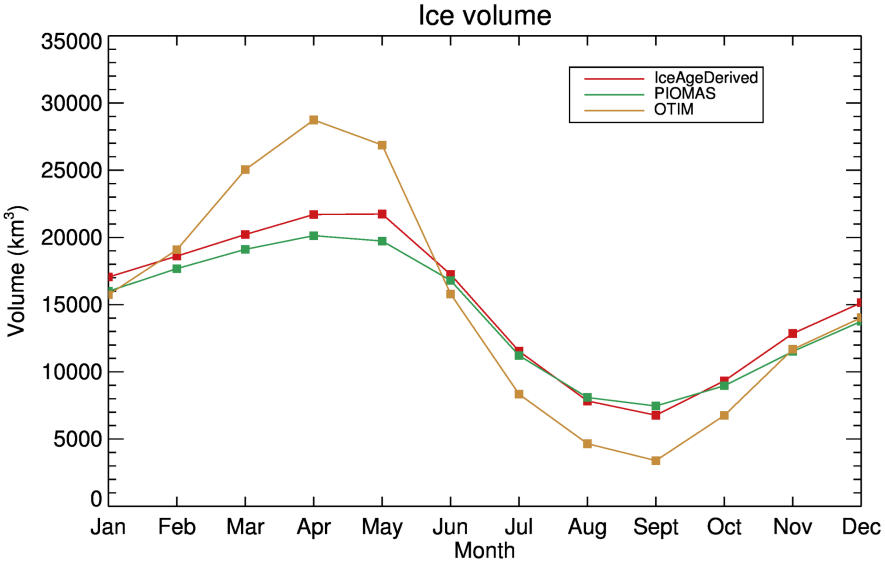

535

Figure 8: Derived climatological mean annual cycle of ice volume 1984-2018 in the Arctic.

https://doi.org/10.5194/tc-2019-192
Preprint. Discussion started: 26 August 2019

The Cryosphere Discussions
Open Access
EGU

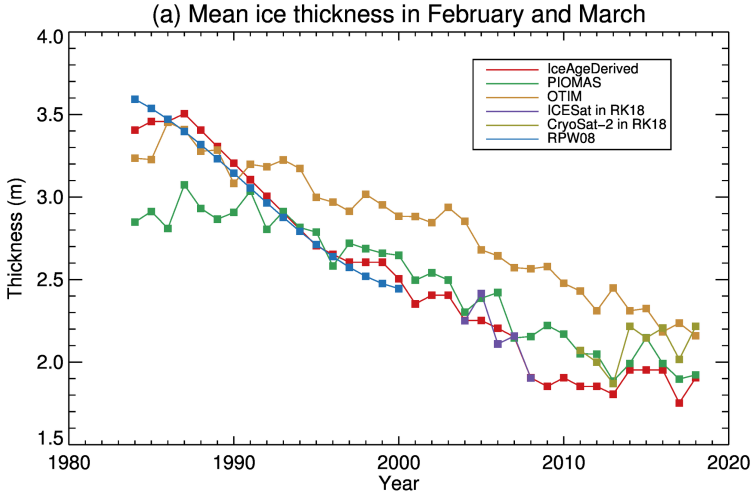

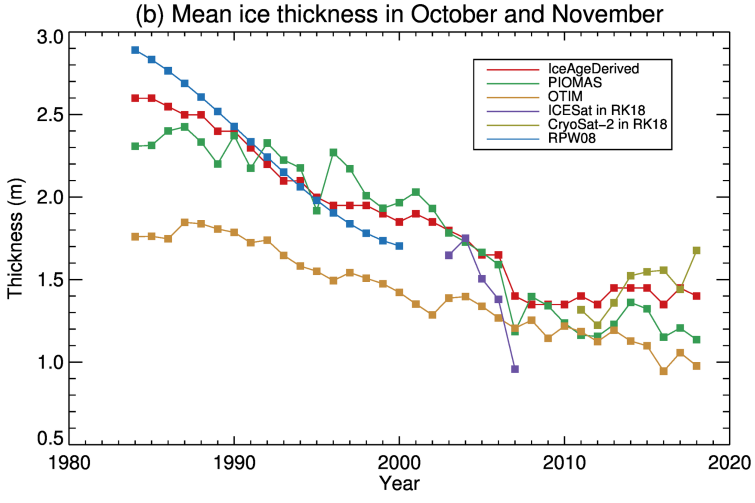

540

Figure 9: Mean ice thickness in GORE box in February and March from 1984 to 2018 derived from ice age, from PIOMAS, from OTIM, and from ICESat (2004-2008) and CryoSat (2011-2018), and submarine data (1984-2000).

https://doi.org/10.5194/tc-2019-192
Preprint. Discussion started: 26 August 2019

The Cryosphere Discussions
Open Access
EGU

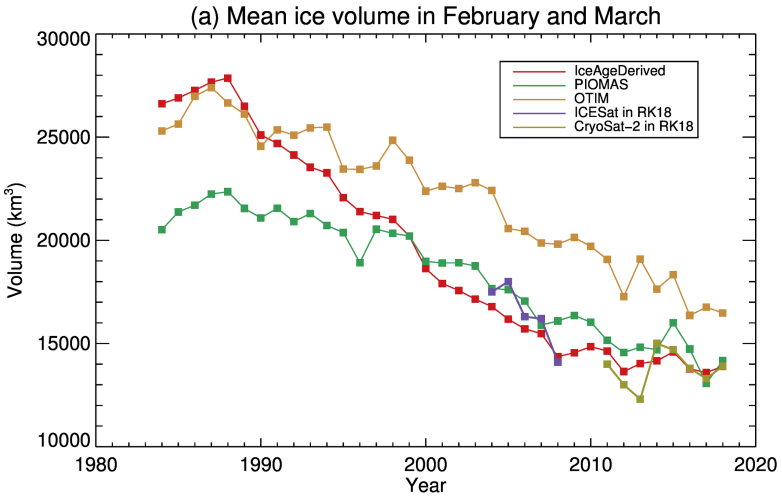

545

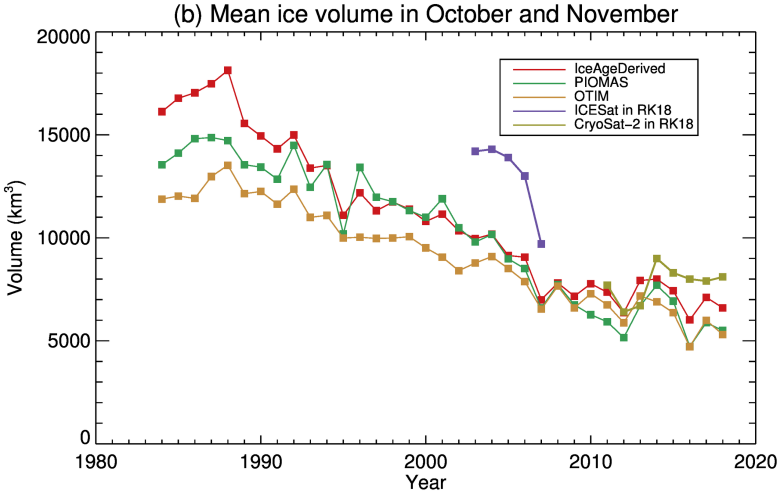

Figure 10: Mean Arctic ice volume in February and March (a) and from October and November (b) from 1984 to 2018 derived from ice age, from PIOMAS, from OTIM, and ICESat (2003-2007) and CryoSat (2011-2018).

https://doi.org/10.5194/tc-2019-192
Preprint. Discussion started: 26 August 2019

550

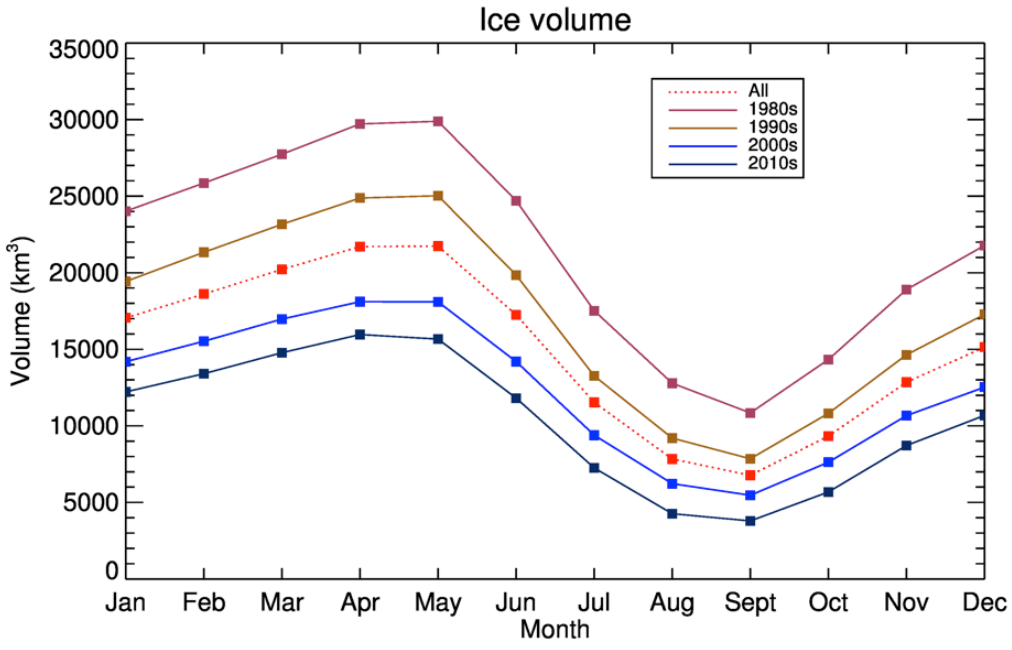

Figure 11: Derived climatological mean annual cycle of ice volume in 1980s, 1990s, 200s, 2010s, and in all years.

https://doi.org/10.5194/tc-2019-192
Preprint. Discussion started: 26 August 2019

The Cryosphere
Discussions
Open Access
EGU

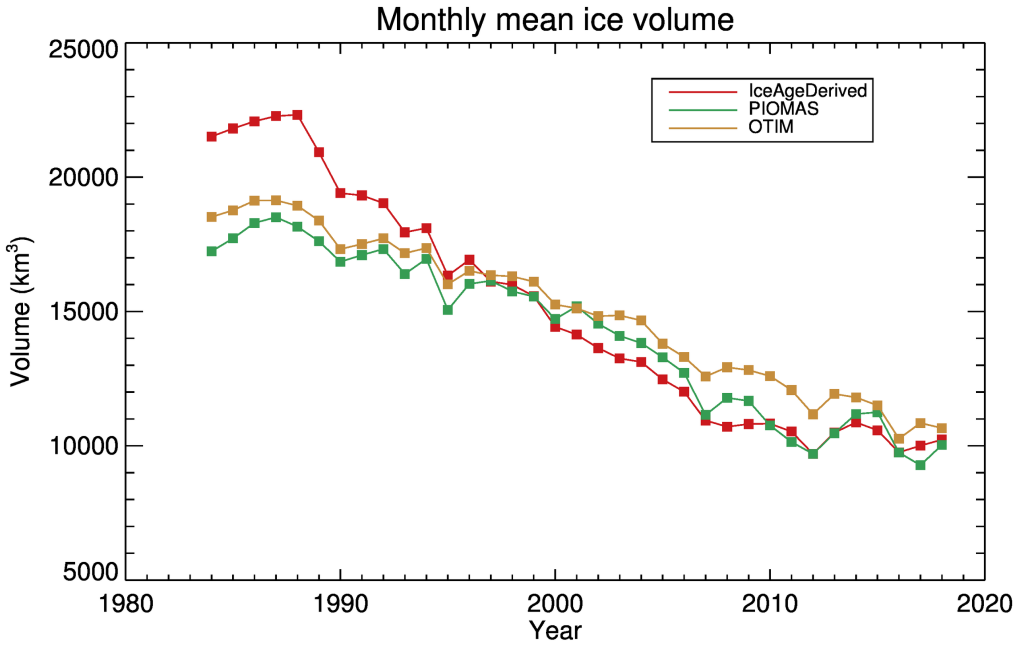

555 **Figure 12: Mean monthly Arctic ice volume from 1984 to 2018 derived from ice age, from PIOMAS, and from OTIM.**

https://doi.org/10.5194/tc-2019-192
Preprint. Discussion started: 26 August 2019

The Cryosphere
Discussions
Open Access
EGU

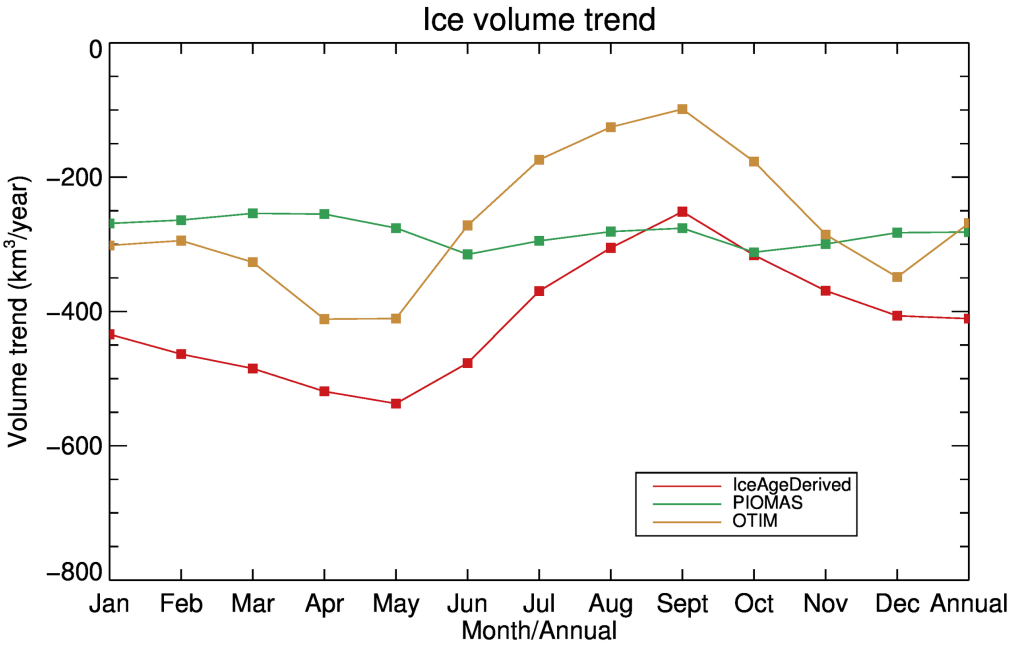

Figure 13: Trend of Arctic ice volume in each month and in annual mean from 1984 to 2018 derived from ice age, from PIOMAS, and from OTIM.

560

https://doi.org/10.5194/tc-2019-192
Preprint. Discussion started: 26 August 2019

The Cryosphere
Discussions
Open Access
EGU

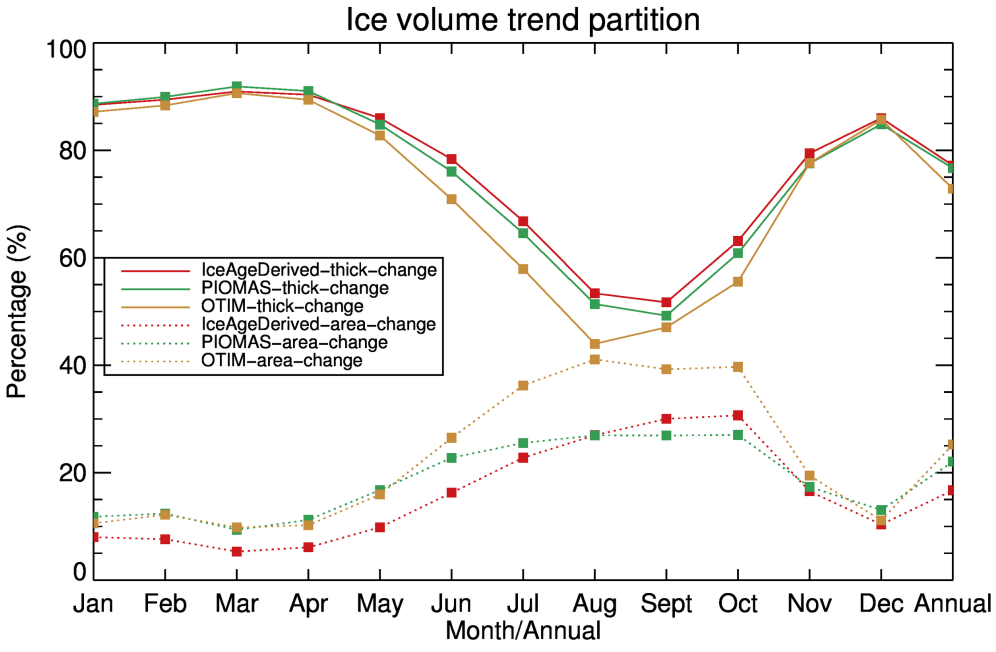

Figure 14: Partition of trend of Arctic ice volume in each month and in annual mean from 1984 to 2018 to changes in ice thickness derived from ice age, from PIOMAS, and from OTIM and ice area.

https://doi.org/10.5194/tc-2019-192
Preprint. Discussion started: 26 August 2019

565 **Appendix**

Table A1. Monthly mean values of the correction term f̃(τ) in Eq.1, from Table 4 in Rothrock et al. (2008).

Month	f̃(τ),m
January	0.087
February	0.098
March	0.110
April	0.118
May	0.122
June	0.113
July	0.026
August	0.004
September	0.025
October	0.054
November	0.070
December	0.081

570

https://doi.org/10.5194/tc-2019-192
Preprint. Discussion started: 26 August 2019

The Cryosphere
Discussions
Open Access
EGU

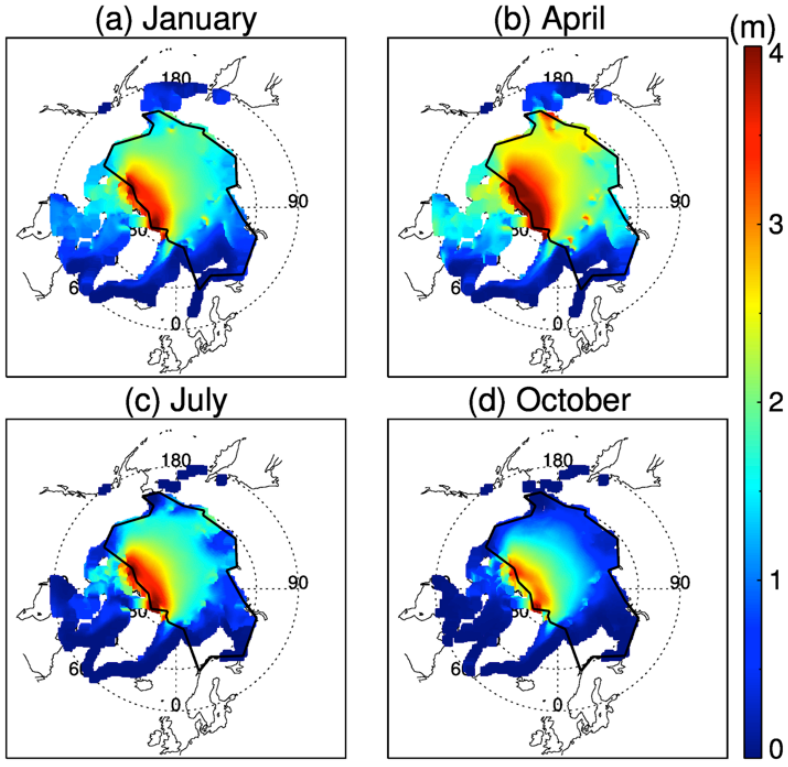

Figure A1: Derived climatological mean sea ice thickness distribution in the Arctic from PIOMAS 1984 t0 2018.

https://doi.org/10.5194/tc-2019-192
Preprint. Discussion started: 26 August 2019

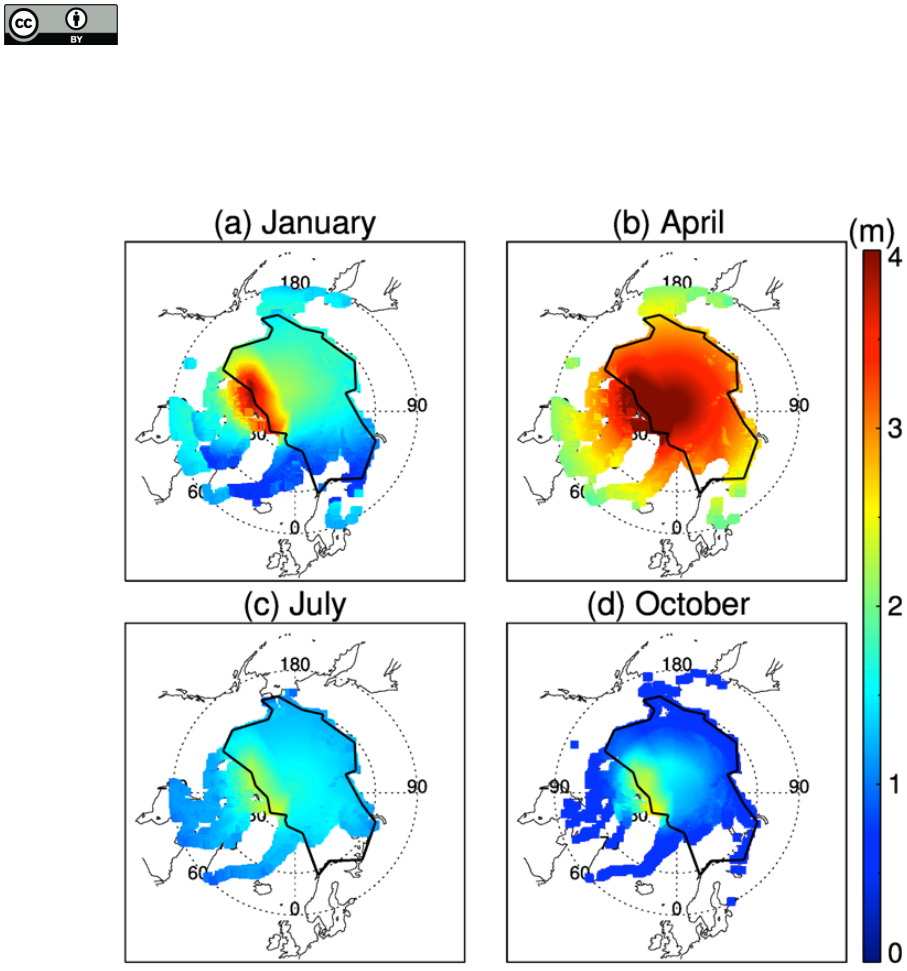

575 **Figure A2: Derived climatological mean sea ice thickness distribution in the Arctic from OTIM 1984 to 2018.**